Peng-fei ZHANG, Yu-kai YAN, Ying LIU, Raj MITTRA, 2020. A look at field manipulation and antenna design using 3D transformation electromagnetics and 2D surface electromagnetics. *Frontiers of Information Technology & Electronic Engineering*, 21(3):351-365. https://doi.org/10.1631/FITEE.1900489

A look at field manipulation and antenna design using 3D transformation electromagnetics and 2D surface electromagnetics

Key words: Field manipulation; Transformation optics; Antenna design; Surface electromagnetics

Corresponding author: Peng-fei ZHANG
E-mail: zhangpf@mail.xidian.edu.cn
ORCID: https://orcid.org/0000-0002-6855-5315

Introduction

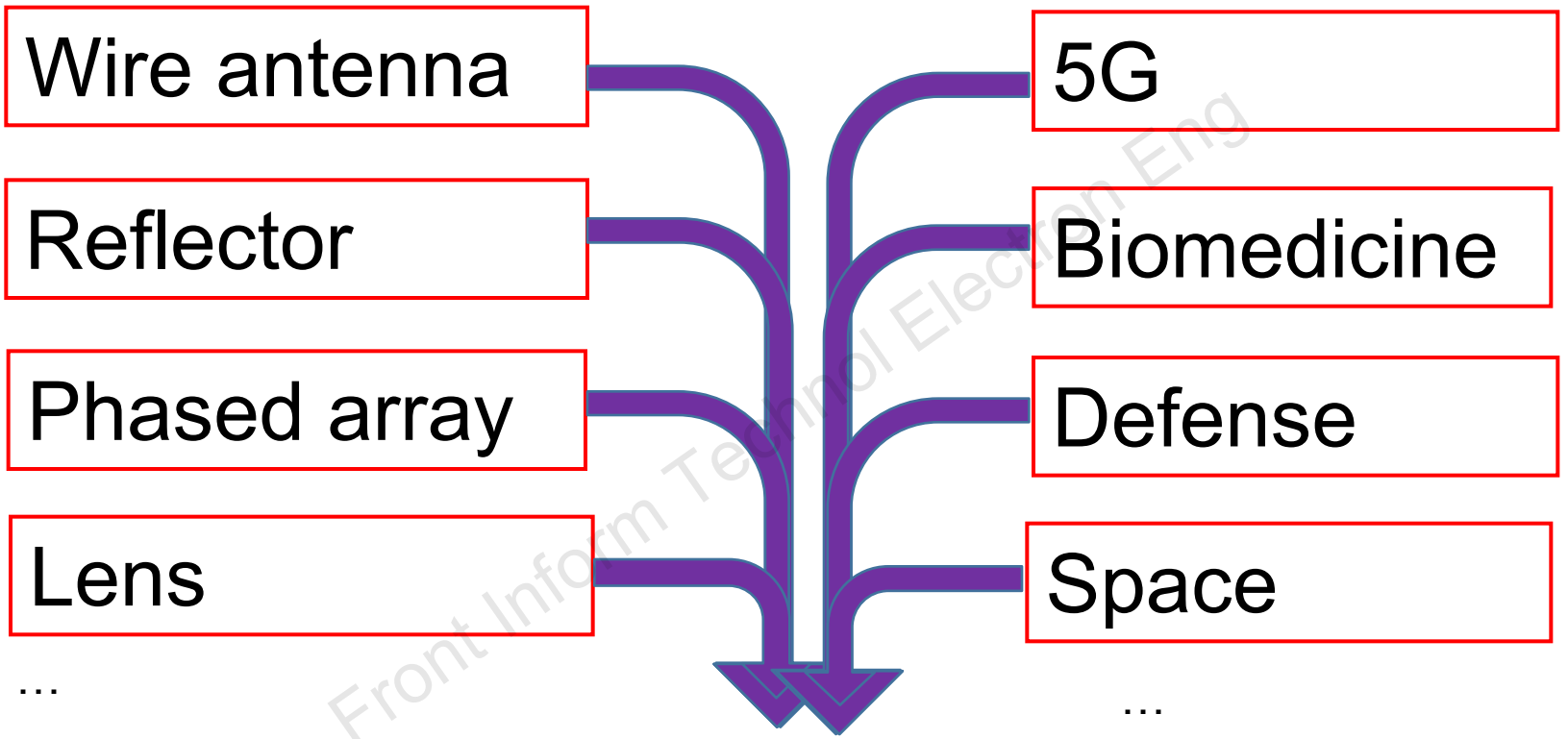

Is it possible to propose general-purpose strategies for the synthesis and design of antennas to achieve the performance characteristics specified by the user?

Introduction

Traditional antenna design

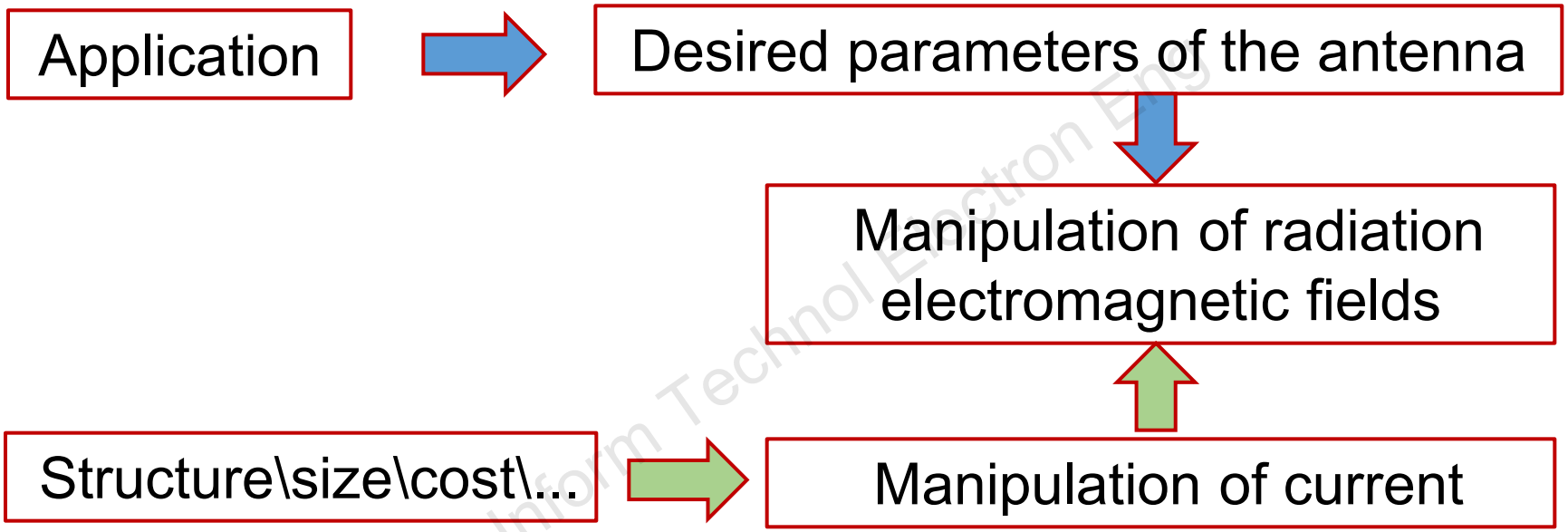

New strategies for antenna design

Introduction

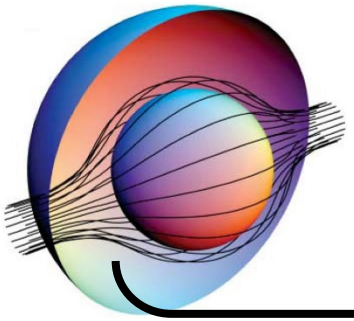

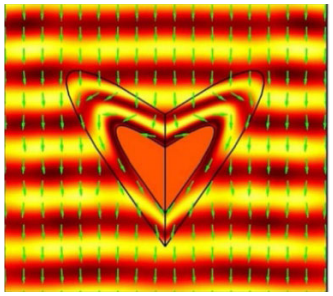

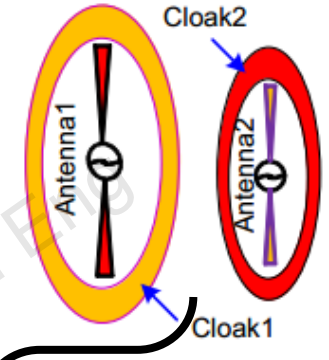

TO

Two possible candidates

SEM

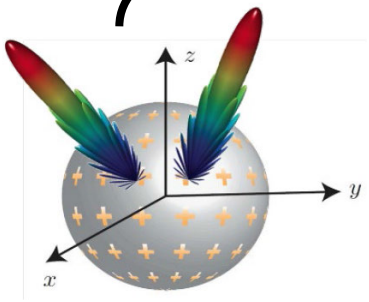

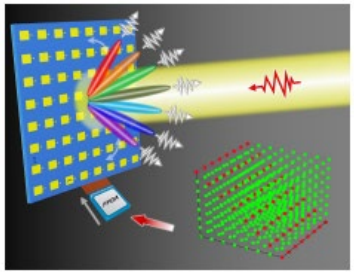

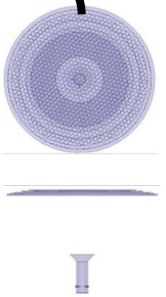

Transformation optics

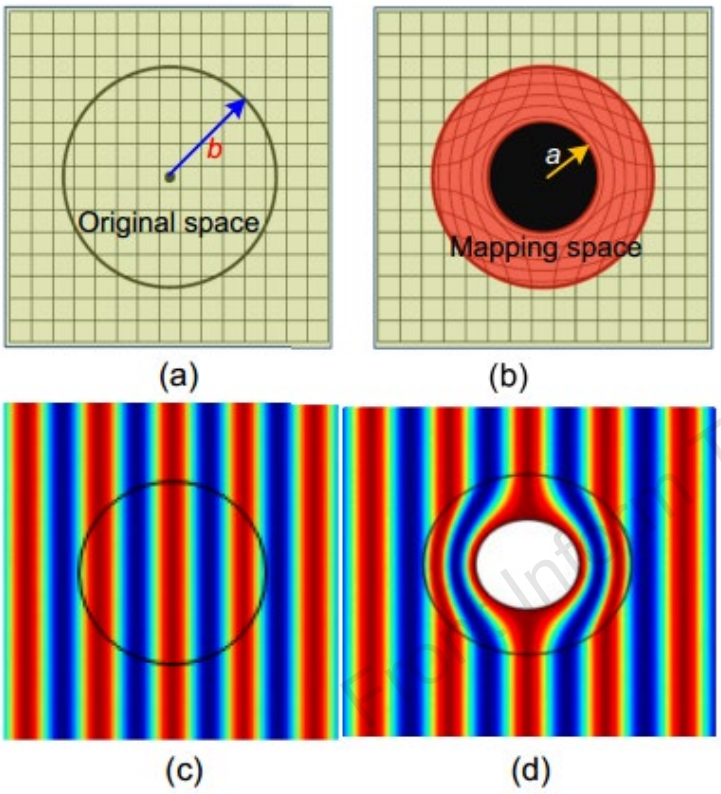

$$\Lambda = \begin{bmatrix} \frac{\partial x'}{\partial x} & \frac{\partial x'}{\partial y} & \frac{\partial x'}{\partial z} \\ \frac{\partial y'}{\partial x} & \frac{\partial y'}{\partial y} & \frac{\partial y'}{\partial z} \\ \frac{\partial z'}{\partial x} & \frac{\partial z'}{\partial y} & \frac{\partial z'}{\partial z} \end{bmatrix}, \Lambda^{-1} = \begin{bmatrix} \frac{\partial x}{\partial x'} & \frac{\partial x}{\partial y'} & \frac{\partial x}{\partial z'} \\ \frac{\partial y}{\partial x'} & \frac{\partial y}{\partial y'} & \frac{\partial y}{\partial z'} \\ \frac{\partial z}{\partial x'} & \frac{\partial z}{\partial y'} & \frac{\partial z}{\partial z'} \end{bmatrix}.$$

$$\begin{cases} [\varepsilon'] = \Lambda[\varepsilon]\Lambda^{\mathrm{T}} / \left|\det \Lambda\right|, \\ [\mu'] = \Lambda[\mu]\Lambda^{\mathrm{T}} / \left|\det \Lambda\right|, \\ \boldsymbol{J}' = \Lambda \boldsymbol{J} / \left|\det \Lambda\right|, \\ \rho' = \rho / \left|\det \Lambda\right|, \end{cases}$$

$$\begin{cases} \boldsymbol{E}' = (\Lambda^{-1})^{\mathrm{T}} \boldsymbol{E}, \quad \boldsymbol{D}' = \Lambda \boldsymbol{D} / \left|\det \Lambda\right|, \\ \boldsymbol{H}' = (\Lambda^{-1})^{\mathrm{T}} \boldsymbol{H}, \quad \boldsymbol{B}' = \Lambda \boldsymbol{B} / \left|\det \Lambda\right|. \end{cases}$$

TO provides an elegant theoretical approach for the electromagnetic field manipulation method by relating the electromagnetic fields in one coordinate system to another. However, it faces the issue of realizing 3D materials and the boundary problem.

New choice of TO

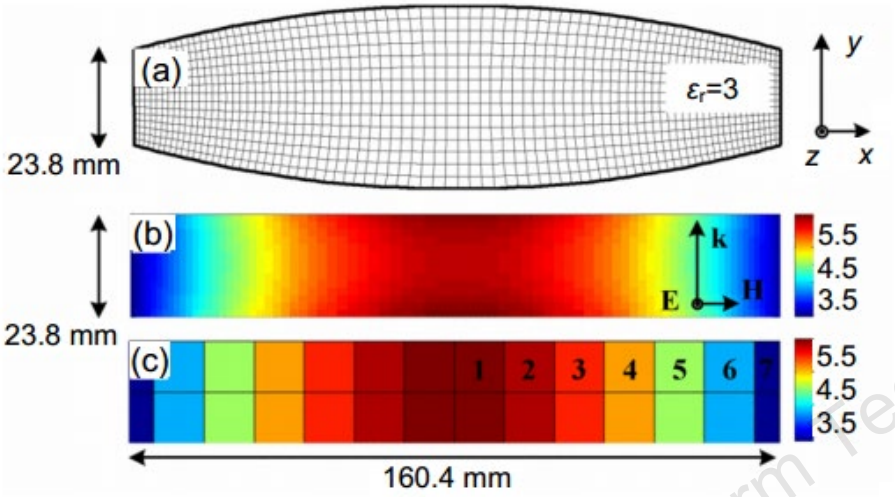

$$\begin{cases} [\varepsilon''] = \dfrac{\zeta}{\xi}\Lambda[\varepsilon]\Lambda^{\mathrm{T}}/\left|\det\Lambda\right|, \\ [\mu''] = \dfrac{\xi}{\zeta}\Lambda[\mu]\Lambda^{\mathrm{T}}/\left|\det\Lambda\right|, \\ \boldsymbol{J}'' = \dfrac{1}{\xi}\Lambda\boldsymbol{J}/\left|\det\Lambda\right|, \\ \rho'' = \dfrac{1}{\xi}\rho/\left|\det\Lambda\right|, \end{cases} \quad \begin{cases} \boldsymbol{E}'' = \dfrac{1}{\zeta}(\Lambda^{-1})^{\mathrm{T}}\boldsymbol{E}, \\ \boldsymbol{H}'' = \dfrac{1}{\xi}(\Lambda^{-1})^{\mathrm{T}}\boldsymbol{H}, \\ \boldsymbol{D}'' = \dfrac{1}{\xi}\Lambda\boldsymbol{D}/\left|\det\Lambda\right|, \\ \boldsymbol{B}'' = \dfrac{1}{\zeta}\Lambda\boldsymbol{B}/\left|\det\Lambda\right|, \end{cases}$$

$$\eta'' = \sqrt{\frac{\mu''}{\varepsilon''}} = \frac{\xi}{\zeta}\eta' = \frac{\xi}{\zeta}\sqrt{\frac{\mu'}{\varepsilon'}} \to \frac{\xi}{\zeta}\sqrt{\frac{\mu_0}{\varepsilon_0}} = \frac{\xi}{\zeta}\eta_0.$$

An appropriate choice of ξ and ζ can modify the impedance of materials located at the central region of the flat lens to avoid the mismatch problem at the interface between the lens and the free space.

Wave-equation-based transformation

$$\left.\begin{aligned} &\nabla^2 E_z + w^2 \mu_0 \varepsilon E_z = 0, \\ &\varepsilon'(x', y') = \varepsilon(x, y)\left|\frac{\mathrm{d}\omega'}{\mathrm{d}\omega}\right|^{-2}, \\ &\nabla'^2 E_z' + w^2 \mu_0 \varepsilon' E_z' = 0. \end{aligned}\right\} \quad E_z'(x', y') = E_z(x, y).$$

This method has the advantage that only isotropic dielectric is required.

Field manipulation based on 2D surface electromagnetics generalized Snell's law

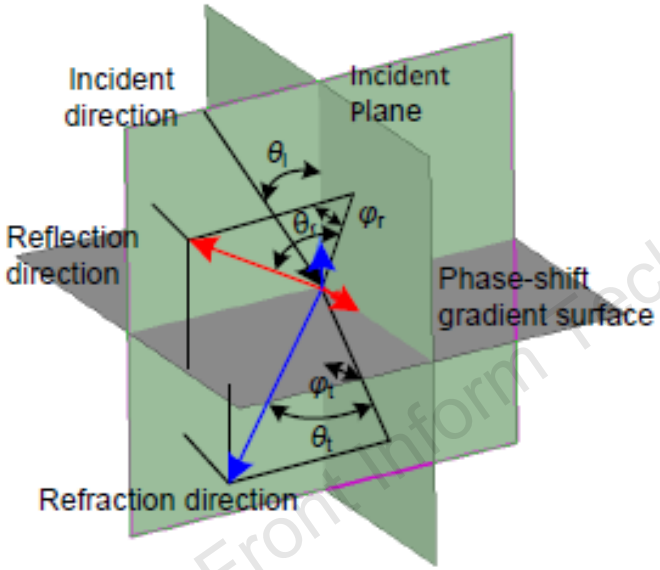

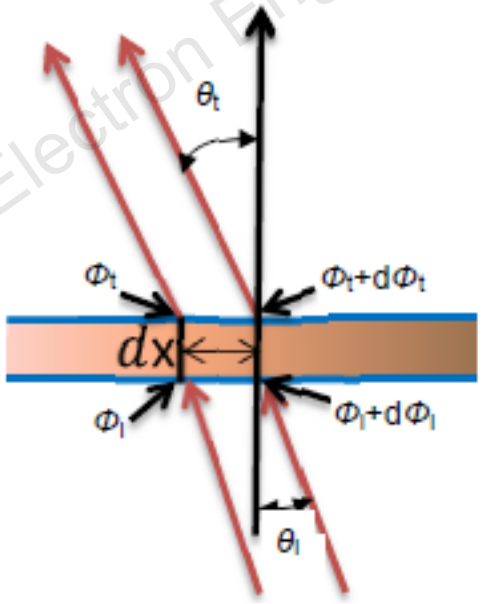

$$\vec{K}_r = \nabla\Phi_r^{\delta} + \vec{K}_i - 2K_0 n_i \hat{n}(\hat{k}_i \bullet \hat{n})$$

$$\vec{K}_t = \nabla\Phi_t^{\delta} + \vec{K}_i - \hat{n}K_0 \left[(n_i \hat{k}_i \bullet \hat{n}) + \sqrt{(n_t)^2 - \left(n_i \left| \hat{k}_i \times \hat{n} \right| \right)^2} \right]$$

New relationship of refraction and critical angles

$$\begin{cases} \varphi_{\mathrm{t}} = \arctan\left(\dfrac{n_{\mathrm{i}} \sin\theta_{\mathrm{i}} \sin\varphi_{\mathrm{i}} + \dfrac{1}{k_0}\dfrac{\partial \Phi_{\mathrm{t}}^{\delta}}{\partial y}}{n_{\mathrm{i}} \sin\theta_{\mathrm{i}} \cos\varphi_{\mathrm{i}} + \dfrac{1}{k_0}\dfrac{\partial \Phi_{\mathrm{t}}^{\delta}}{\partial x}} \right), \\ \theta_{\mathrm{t}} = \arcsin\left\{ \dfrac{1}{n_{\mathrm{t}}} \left[\left(n_{\mathrm{i}} \sin\theta_{\mathrm{i}} \cos\varphi_{\mathrm{i}} + \dfrac{1}{k_0}\dfrac{\partial \Phi_{\mathrm{t}}^{\delta}}{\partial x} \right)^2 + \left(n_{\mathrm{i}} \sin\theta_{\mathrm{i}} \sin\varphi_{\mathrm{i}} + \dfrac{1}{k_0}\dfrac{\partial \Phi_{\mathrm{t}}^{\delta}}{\partial y} \right)^2 \right]^{\frac{1}{2}} \right\}. \end{cases} \tag{22}$$

$$\left[\left(n_{\mathrm{i}} \sin\theta'_{\mathrm{c,i}} \cos\varphi_{\mathrm{i}} + \frac{1}{k_0}\frac{\partial \Phi_{\mathrm{t}}^{\delta}}{\partial x} \right)^2 + \left(n_{\mathrm{i}} \sin\theta'_{\mathrm{c,i}} \cos\varphi_{\mathrm{i}} + \frac{1}{k_0}\frac{\partial \Phi_{\mathrm{t}}^{\delta}}{\partial y} \right)^2 \right]^{\frac{1}{2}} = n_{\mathrm{t}}. \tag{23}$$

New relationship of reflection and critical angles

$$\begin{cases} \varphi_{\mathrm{r}} = \arctan\left(\dfrac{n_{\mathrm{i}} \sin\theta_{\mathrm{i}} \sin\varphi_{\mathrm{i}} + \dfrac{1}{k_0}\dfrac{\partial \Phi_{\mathrm{r}}^{\delta}}{\partial y}}{n_{\mathrm{i}} \sin\theta_{\mathrm{i}} \cos\varphi_{\mathrm{i}} + \dfrac{1}{k_0}\dfrac{\partial \Phi_{\mathrm{r}}^{\delta}}{\partial x}} \right), \\ \theta_{\mathrm{r}} = \arcsin\left[\left(\sin\theta_{\mathrm{i}} \cos\varphi_{\mathrm{i}} + \dfrac{1}{n_{\mathrm{i}}}\dfrac{1}{k_0}\dfrac{\partial \Phi_{\mathrm{r}}^{\delta}}{\partial x} \right)^2 + \left(\sin\theta_{\mathrm{i}} \sin\varphi_{\mathrm{i}} + \dfrac{1}{n_{\mathrm{i}}}\dfrac{1}{k_0}\dfrac{\partial \Phi_{\mathrm{r}}^{\delta}}{\partial y} \right)^2 \right]^{\frac{1}{2}}. \end{cases} \tag{25}$$

$$\left[\left(\sin\theta_{\mathrm{i}} \cos\varphi_{\mathrm{i}} + \frac{1}{n_{\mathrm{i}}}\frac{1}{k_0}\frac{\partial \Phi_{\mathrm{r}}^{\delta}}{\partial x} \right)^2 + \left(\sin\theta_{\mathrm{i}} \sin\varphi_{\mathrm{i}} + \frac{1}{n_{\mathrm{i}}}\frac{1}{k_0}\frac{\partial \Phi_{\mathrm{r}}^{\delta}}{\partial y} \right)^2 \right]^{\frac{1}{2}} = 1. \tag{26}$$

Antenna design examples based on field manipulation

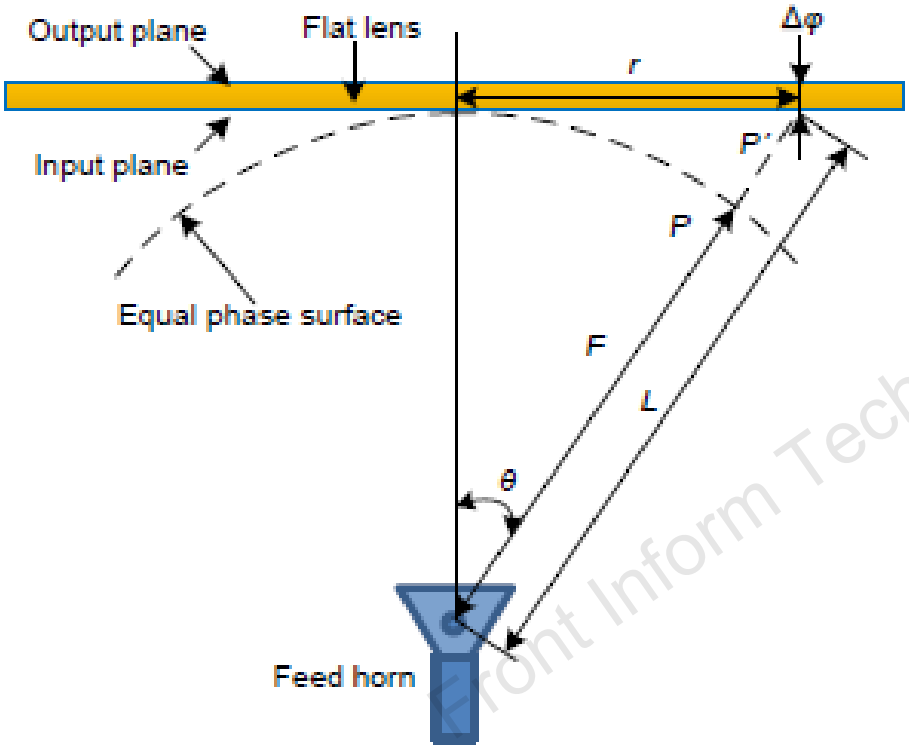

Fig. 5 Flat lens antenna with high gain

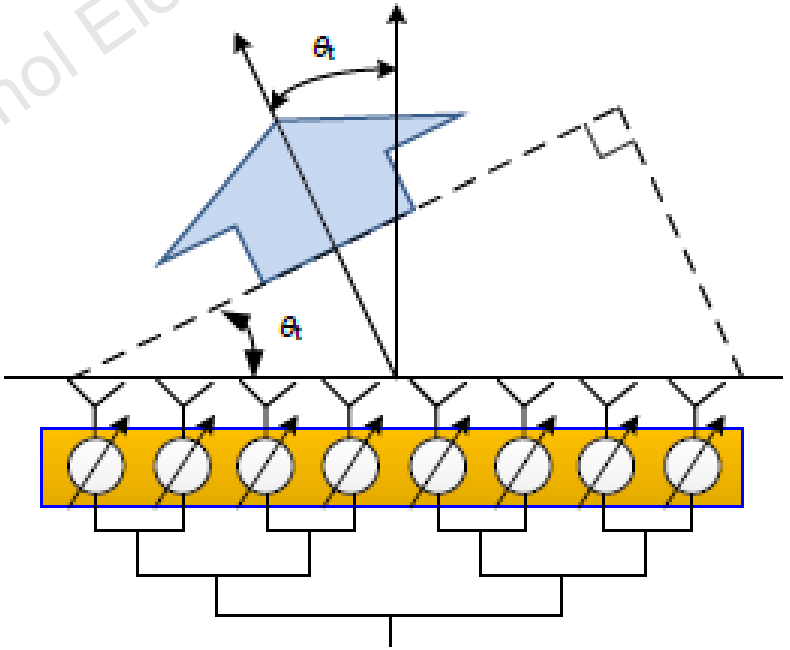

Fig. 6 Schematic used to show the principles of the phased array

Antenna design examples based on field manipulation

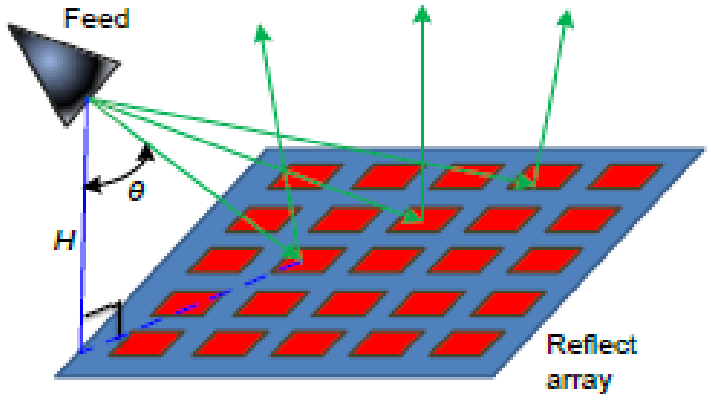

Fig. 7 Schematic used to show the principles of the reflect array

Reprinted from Zhang PF et al. (2017), Copyright 2017, with permission from IEEE

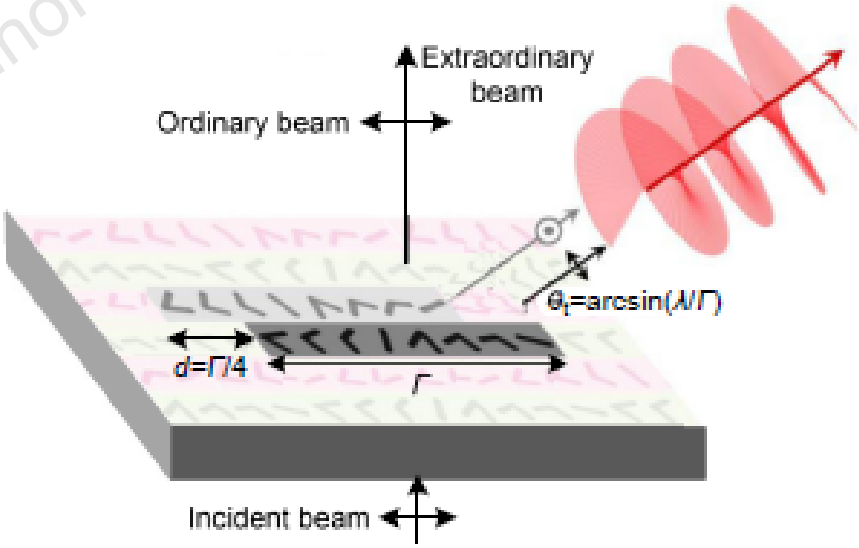

Fig. 8 Schematic showing the working mechanism of a metasurface to generate orbital angular momentum

Antenna design examples based on field manipulation

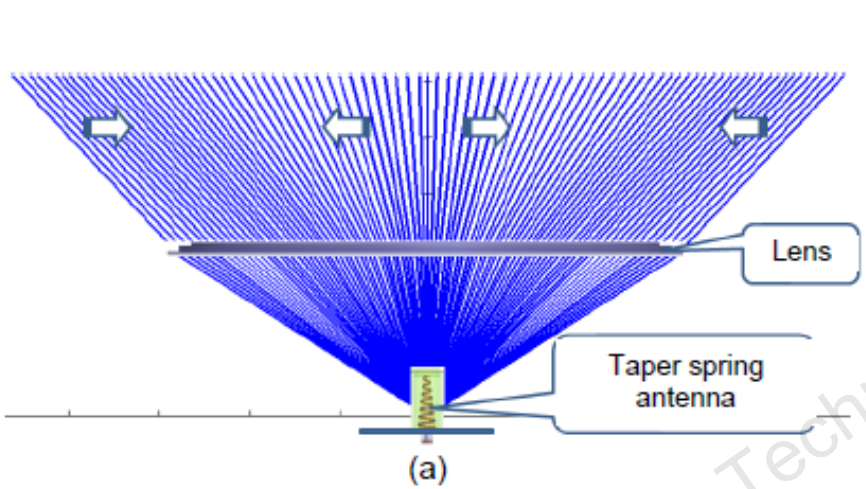

(a)

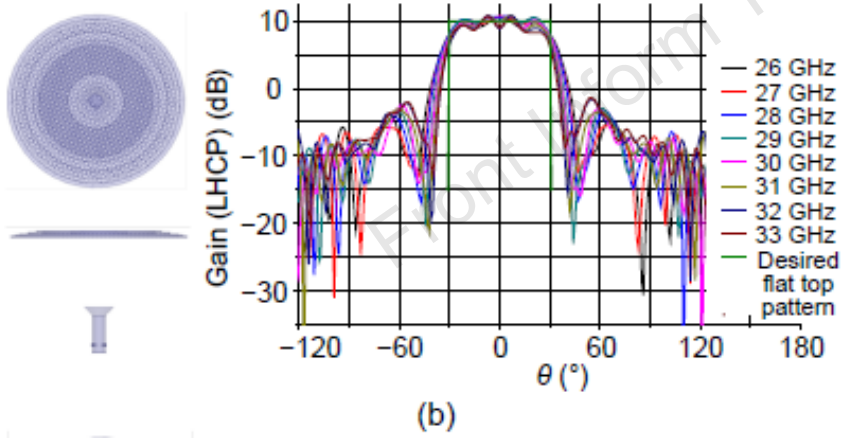

(b)

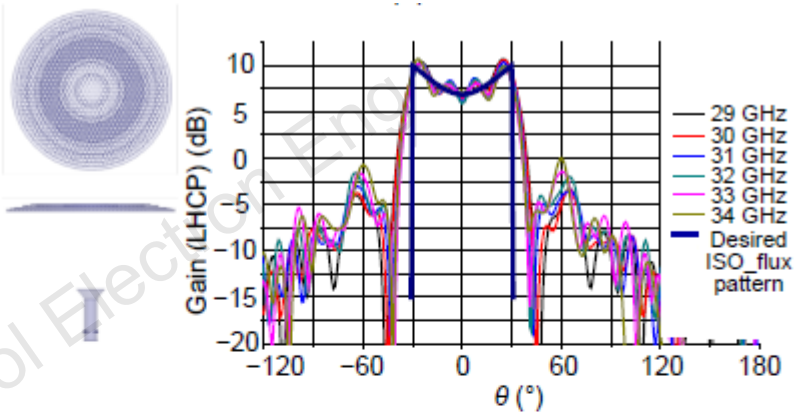

(c)

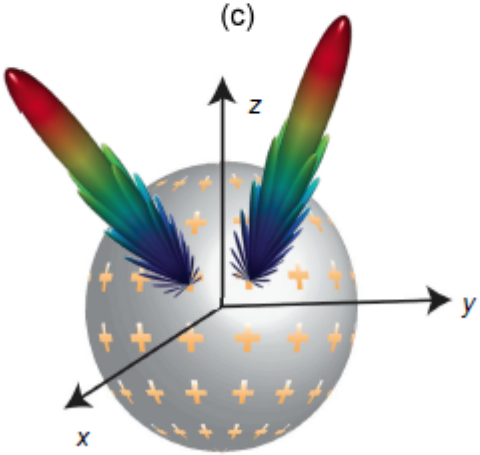

(d)

Fig. 9 Beam shaping based on GSL: (a) ray trace; (b) lens and flat top beam; (c) lens and ISO_flux beam; (d) metasurface generating a simultaneous multi-beam

Antenna design examples based on field manipulation

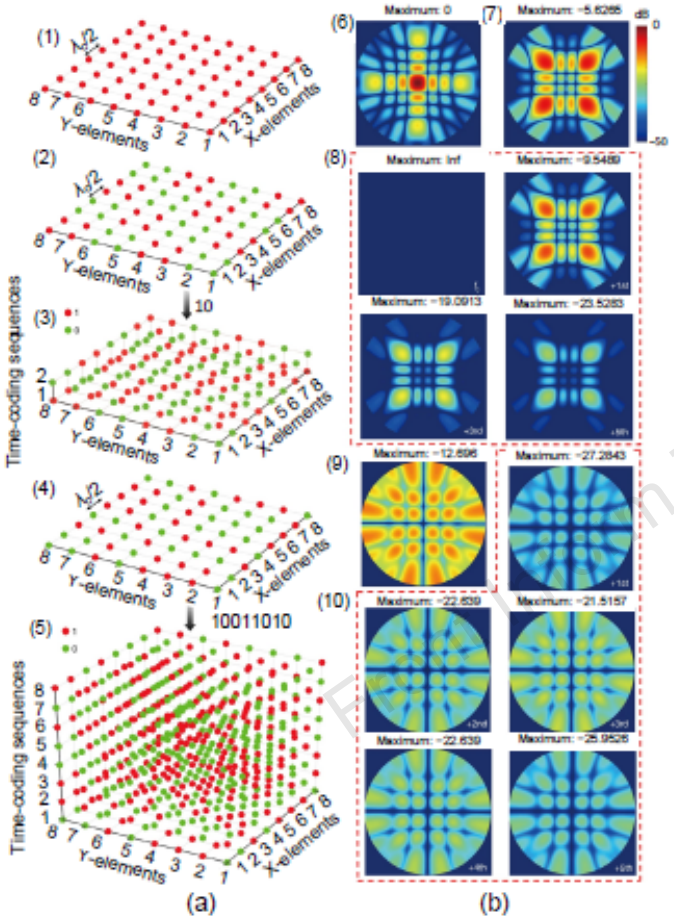

Fig. 11 Radar cross section (RCS) reductions via space-time-coding metasurfaces: (a) development of space-time-coding; (b) scattering patterns at different harmonic frequencies pertaining to different space-time-coding strategies

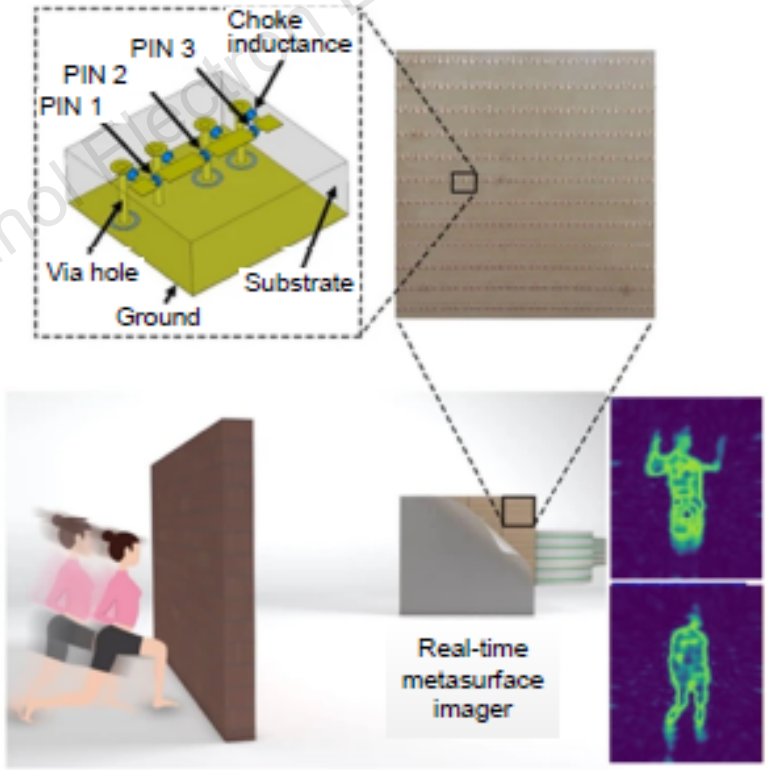

Fig. 12 Illustration of a real-time reprogrammable metasurface imager imaging a moving person behind a wall

Antenna design examples based on field manipulation

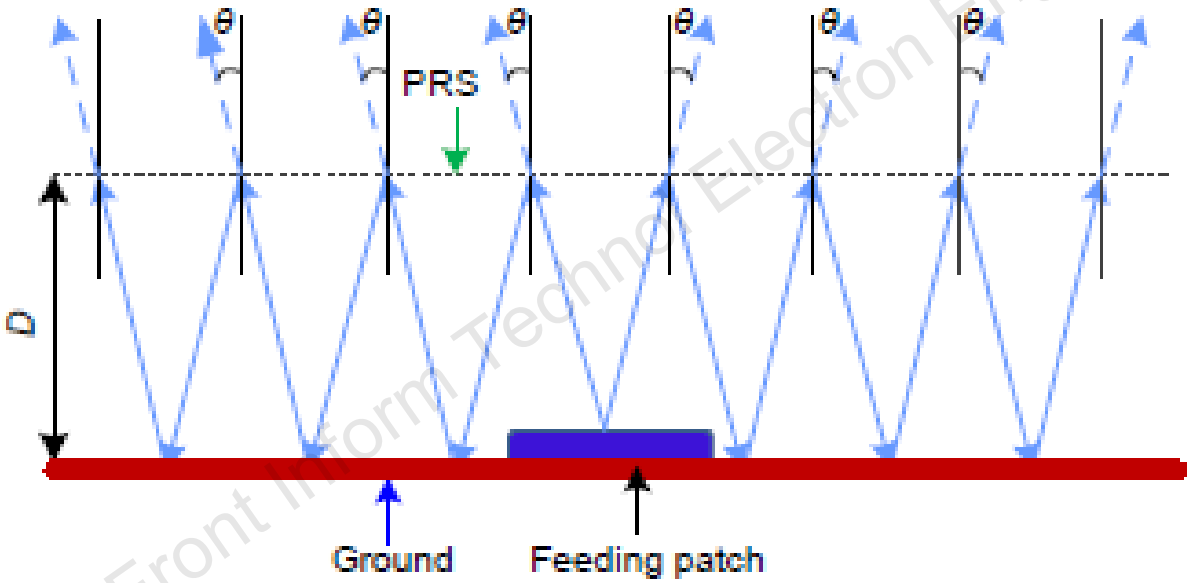

Fig. 13 Model of the Fabry-Perot cavity antenna with partially reflecting surfaces (PRS)

Antenna design examples based on field manipulation

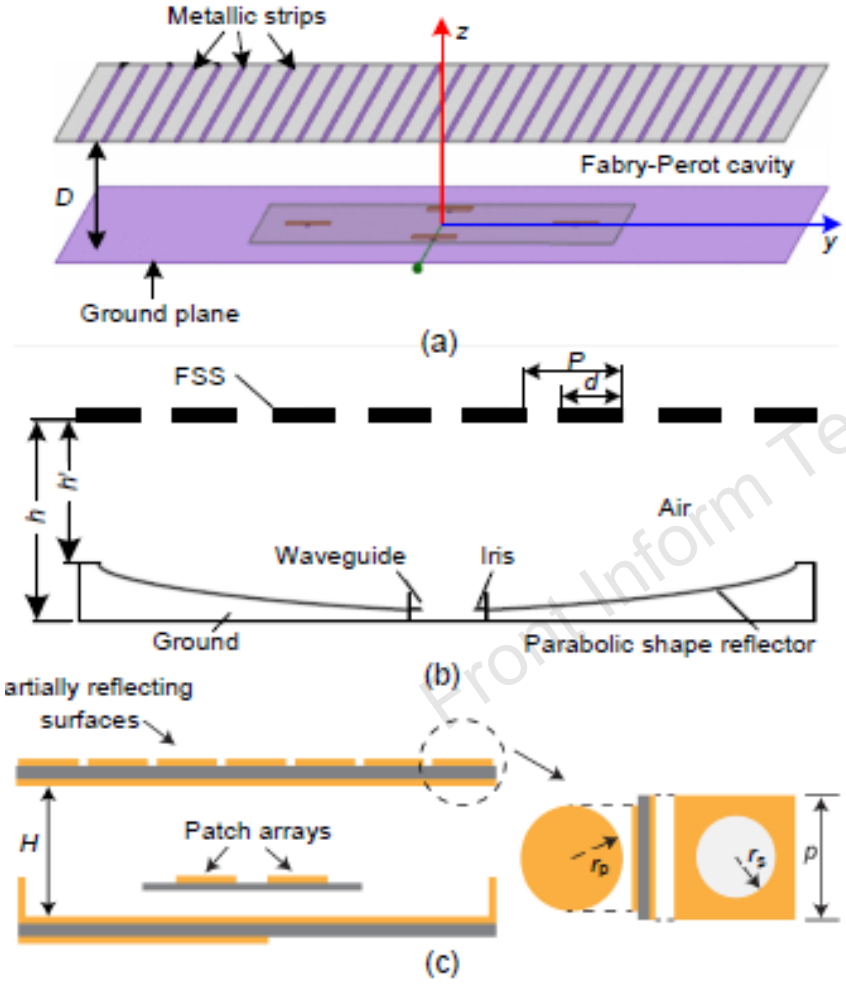

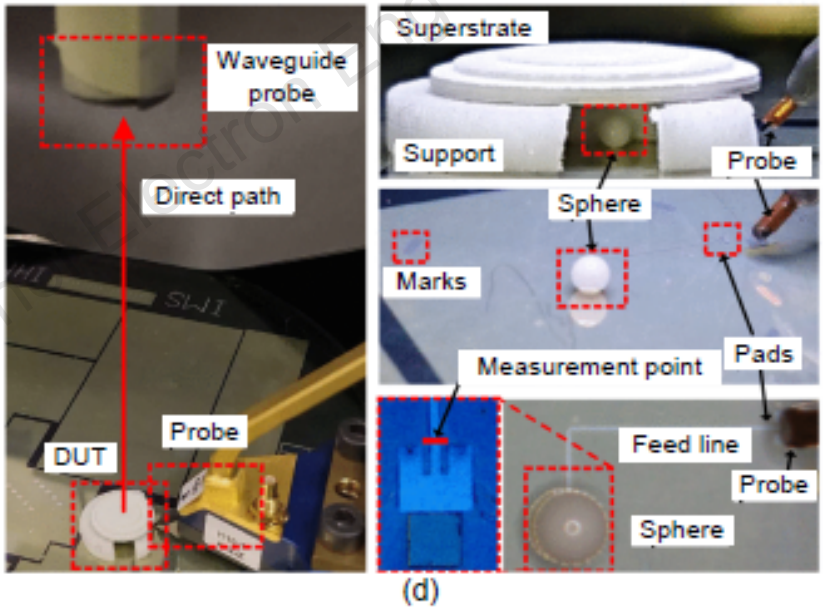

Fig. 14 Multi-feed Fabry-Perot cavity antenna (FPCA) (a), broadband FPCA with a parabolic shape reflector (b), reconfigurable FPCA (Lian et al., 2017) (c), and FPCA with multilayered dielectric sheets (Marin et al., 2019) (d)

Performing mathematical operation with field manipulation

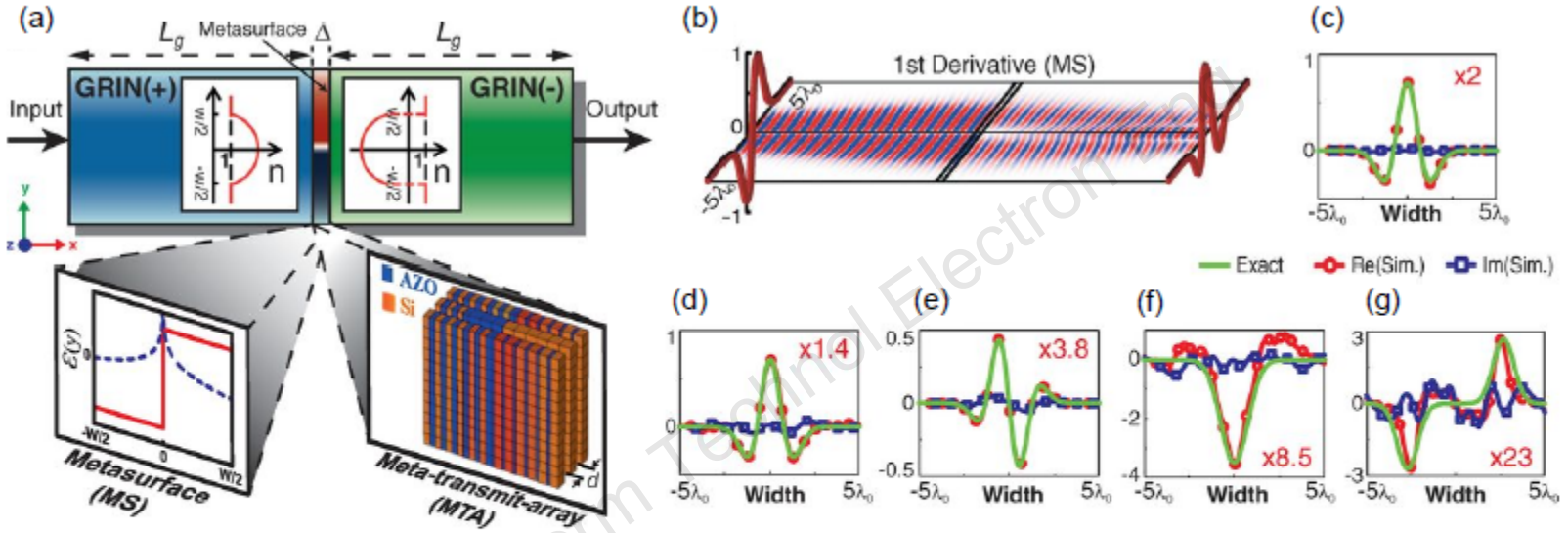

Fig. 15 Metamaterial computing using metasurfaces: (a) illustration of metamaterial computing using metasurfaces; (b) perspective views of the input and output functions; (c) simulation results of metamaterial computing using metamaterial for the first differentiation of the input function; (d) simulation results of metamaterial computing using meta-transmit-array for the first differentiation of the input function; (e) simulation results of metamaterial computing using metamaterial for the second differentiation of input function; (f) simulation results of the second differentiation operation; (g) simulation results of the convolution operation

This example provides another model for combining 3D field manipulation within GRIN and 2D manipulation using a metasurface. If the mathematical operation performance can be integrated into the antenna system within the framework of field manipulation, the antenna may play a more powerful role in the future.

Conclusions

1. We have presented two different field manipulation techniques, i.e., 3D transformation electromagnetics and 2D surface electromagnetics, and their applications in antenna design. Our primary motivation has been to see if we could develop a robust and general-purpose tool for innovative design of antennas for future communication.

2. Our primary emphasis has been to lay the foundations of the theoretical aspects of various field manipulation techniques. Although we have mentioned a variety of applications of field manipulation techniques, most of the designs presented herein have not been realized.

3. It is our sincere hope that researchers in the area will vigorously pursue this aspect of the research, and help bridge the gap that exists today between the theory and practice of the field manipulation techniques, either for designing real-word antennas for novel applications in the future, or for realizing improvements of the performance of existing antennas.